

cGANs with Conditional Convolution Layer

Min-Cheol Sagong · Yong-Goo Shin · Yoon-Jae Yeo · Seung Park ·
Sung-Jea Ko

Received: date / Accepted: date

Abstract Conditional generative adversarial networks (cGANs) have been widely researched to generate class conditional images using a single generator. However, in the conventional cGANs techniques, it is still challenging for the generator to learn condition-specific features, since a standard convolutional layer with the same weights is used regardless of the condition. In this paper, we propose a novel convolution layer, called the conditional convolution layer, which directly generates different feature maps by employing the weights which are adjusted depending on the conditions. More specifically, in each conditional convolution layer, the weights are conditioned in a simple but effective way through filter-wise scaling and channel-wise shifting operations. In contrast to the conventional methods, the proposed method with a single generator can effectively handle condition-specific characteristics. The experimental results on CIFAR, LSUN and ImageNet datasets show that the generator with the proposed conditional convolution layer achieves a higher quality of conditional

image generation than that with the standard convolution layer.

Keywords Deep learning · Generative adversarial networks · Conditional image generation

1 Introduction

Generative adversarial networks (GANs) [5] have brought about remarkable improvements to image generation algorithms. In general, GANs consist of a generator and a discriminator which are trained with competing goals. The generator is trained to mimic the target data distribution, while the discriminator is optimized to differentiate between real and generated samples [1, 27]. As an extension of the GANs, various conditional GANs (cGANs) techniques have been proposed to generate class-conditional samples [1, 13, 20]. Early research into cGANs typically provide the conditional information to both the generator and the discriminator by naively concatenating that information to the input image or some intermediate layers [13, 17, 19], or by adopting the conditional batch-normalization (cBN) [4]. These strategies have shown promising results and have been successfully applied to various image processing techniques including style transfer [4, 8], text-to-image synthesis [19, 20, 27], and image-to-image transformation [10, 29]. Recently, Miyato *et al.* [15] proposed a novel cGANs framework which significantly improves the visual quality as well as the diversity of the generated image by applying a projection discriminator. In the conventional cGANs techniques, however, it is still difficult to build an efficient generator learning condition-specific features.

The primary motivation for the proposed work is as follows: most cGANs frameworks build a generator with stacks of standard convolution, cBN [4], and activation

Min-Cheol Sagong
Korea university
E-mail: mcsagong@dali.korea.ac.kr

Yong-Goo Shin
Korea university
E-mail: ygshin@dali.korea.ac.kr

Yoon-Jae Yeo
Korea university
E-mail: yjyeo@dali.korea.ac.kr

Seung Park
Korea university
E-mail: spark@dali.korea.ac.kr

Sung-Jea Ko
Korea university
E-mail: sjko@korea.ac.kr

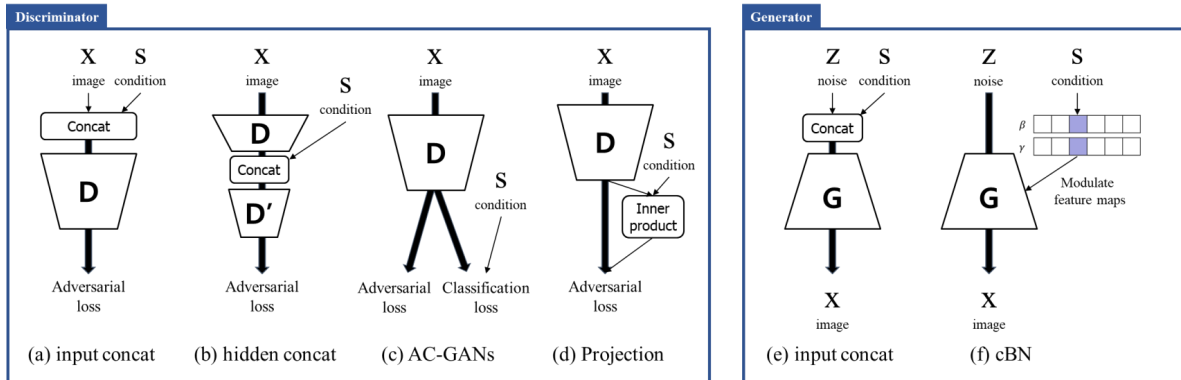


Fig. 1 Various models of the generator and discriminator for cGANs. (a) the discriminator concatenating the one-hot conditional vector to the input image, (b) the discriminator concatenating the one-hot conditional vector to the intermediate layer, (c) the discriminator with the auxiliary loss, (d) the projection discriminator [15], (e) the generator concatenating the one-hot conditional vector to the input noise vector, (f) the generator with the conditional normalization layer

layers. In order to produce the conditioned activation, these stacks modulate the convolutional feature maps in the cBN layer in which the parameters are inferred from the given class. However, it is often difficult to effectively handle the condition-specific characteristics in the activation due to the sharing parameters, regardless of the condition, of the convolution layer. The intuitive way to process the conditioned activation without sharing parameters is to build the same number of generators as the condition; however, this approach requires not only considerable memory but also time for training.

In this paper, we propose a novel convolution layer, called a conditional convolution layer (cConv), which uses different weights depending on the given class. More specifically, in each cConv, the weights are conditioned in a simple but effective way through filter-wise scaling and channel-wise shifting operations. The filter-wise scaling adjusts each filter of cConv using specialized scaling parameters to a specific condition, whereas the channel-wise shifting modulates each channel of the filters with different shifting parameters. Unlike with conventional methods, the proposed method can directly process the condition-specific features without a cBN layer. We conducted extensive experiments on several datasets including CIFAR [23], LSUN [25] and tiny-ImageNet [3, 24] to demonstrate the effectiveness of the proposed method. We show that with the help of the proposed cConv, a single generator can produce conditional images with higher-quality than the state-of-the-art methods. We also performed additional experiments which combine the cConv with conventional conditioning techniques such as the cBN to validate the effectiveness of the cConv. In order to prove the generalization ability of cConv, we further applied the cConv

to the conditional style-transfer network and succeeded in adjusting images with various styles of art paintings.

In summary, this paper makes three major contributions. (i) We propose a novel conditional convolution layer which produces different feature maps by using the specialized weights according to the particular conditions. Armed with cConv, the generator achieves higher performance in generating conditional images than the conventional methods. (ii) We introduce the sequential operations of filter-wise scaling and channel-wise shifting which adjust the weights depending on the given class with a small number of parameters. (iii) We extend the application of cConv to the conditional style-transfer and successfully produce visually pleasing results.

In the rest of this paper, we first introduce related work and preliminaries in Section 2 and Section 3. Then, we discuss the proposed cConv in Section 4. In Section 5, extensive experimental results are introduced to demonstrate that the proposed method outperforms conventional methods on various datasets. Finally, we describe our conclusion in Section 6.

2 Related work

The cGANs are one of the groups of GANs, and they generate images with the given class [13]. Unlike with the standard GANs, both the generator and the discriminator of the cGANs require conditional information to generate class-conditional images and differentiate them from the target class. To this end, as shown in Fig. 1, various methods have been proposed to effectively provide the conditional information for both networks [4, 8, 9, 13–17, 19–21]. Earlier methods have provided the conditional information by concatenating the class label (one-hot vector) into the input im-

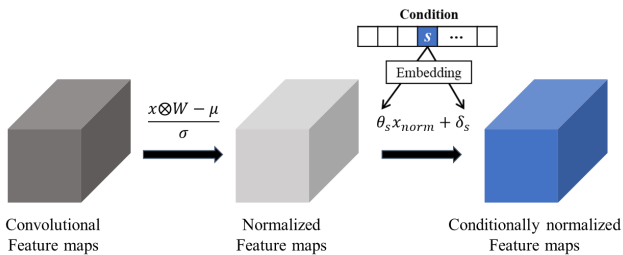


Fig. 2 Simplified diagram of the cBN. The convolutional feature maps obtained through convolution operation are first normalized with mean μ and standard deviation σ , and then normalized feature maps are modulated using condition-specific scaling and shifting parameters.

age or intermediate layers for the discriminator [13, 19] as depicted in Fig. 1(a) and (b). Reed *et al.* [20] improved upon these frameworks by building richer conditional information such as a target bounding box. On the other hand, some researchers [16, 17, 21] have proposed a modified discriminator with an auxiliary classification network, which is trained to predict the class label of the input image as well as differentiate between the real and fake samples, as shown in Fig. 1(c). Recently, inspired by probabilistic models, Miyato *et al.* [15] proposed the projection discriminator. As depicted in Fig. 1(d), the projection discriminator takes an inner product between the embedded condition vector and the feature vector of the discriminator so as to impose a regularity condition. Along with significantly improving the visual quality, the projection discriminator also guarantees the diversity of the generated images.

Meanwhile, a few attempts have been made to process the conditional information for the generator. Typically, the earlier works [13, 17, 19] provided the conditional information to the generator by concatenating the class label into an input noise vector as shown in Fig. 1(e). However, the performance of this approach is fundamentally limited due to the handling of the conditional information only in the first layer of the generator. In order to alleviate this problem, as shown in Fig. 1(f), some studies proposed conditional normalization layers which supply intermediate layers with the conditional information [4, 8]. Despite the fact that these methods can differently modulate the convolutional feature maps according to the conditions, they cannot overcome the major problem that the common weights are employed without regard to the classes.

3 Preliminaries

3.1 Conditional generative adversarial network

The GANs have been improved upon since they were first introduced by Goodfellow *et al.* [5]. In the GANs, the generator G is trained to create fake images which are indistinguishable from real ones, while the discriminator D is trained to classify between real and generated images. This competing training is defined as

$$\min_G \max_D E_{I \sim P_{\text{data}}(I)} [\log D(I)] + E_{z \sim P_z(z)} [\log(1 - D(G(z)))], \quad (1)$$

where z and I represent a random noise vector and a real image sampled from noise distribution $P_z(z)$ and target distribution $P_{\text{data}}(I)$, respectively. More recently, cGANs, which focus on producing the class conditional images, have been actively researched [13, 14, 17, 28]. In general, cGANs techniques add the conditional information s , such as class labels or text condition, to both generator and discriminator in order to control the data generation process in a supervised manner. This can be formally expressed as follows:

$$\min_G \max_D E_{(I,s) \sim P_{\text{data}}(I)} [\log D(I, s)] + E_{z \sim P_z(z), s \sim P_{\text{data}}(s)} [\log(1 - D(G(z, s)))]. \quad (2)$$

Using the above equation, the cGANs can select an image category to be generated, which is not possible when using the standard GANs framework.

3.2 Conditional normalization layer

The conditional normalization layer including the adaptive instance normalization [8] and the cBN [4] is considered to be an important component in the cGANs frameworks. In particular, the cBN is widely used to provide the conditional information to the generator [14, 15]. Unlike the standard normalization layers, as shown in Fig. 2, the cBN requires external conditional information which determines the condition-specific scaling and shifting parameters. The cBN operates as follows: First, the convolutional feature maps obtained through the convolution operation are normalized with mean μ and standard deviation σ in the same way as the batch normalization process. Then, the normalized feature maps are scaled and shifted using a learned affine transformation whose parameters are specialized to the conditional information. Formally, the cBN with standard convolution layer can be expressed as follows:

$$f_{\text{cBN}}(x, s) = \theta_s \left(\frac{x \otimes W - \mu}{\sigma} \right) + \delta_s, \quad (3)$$

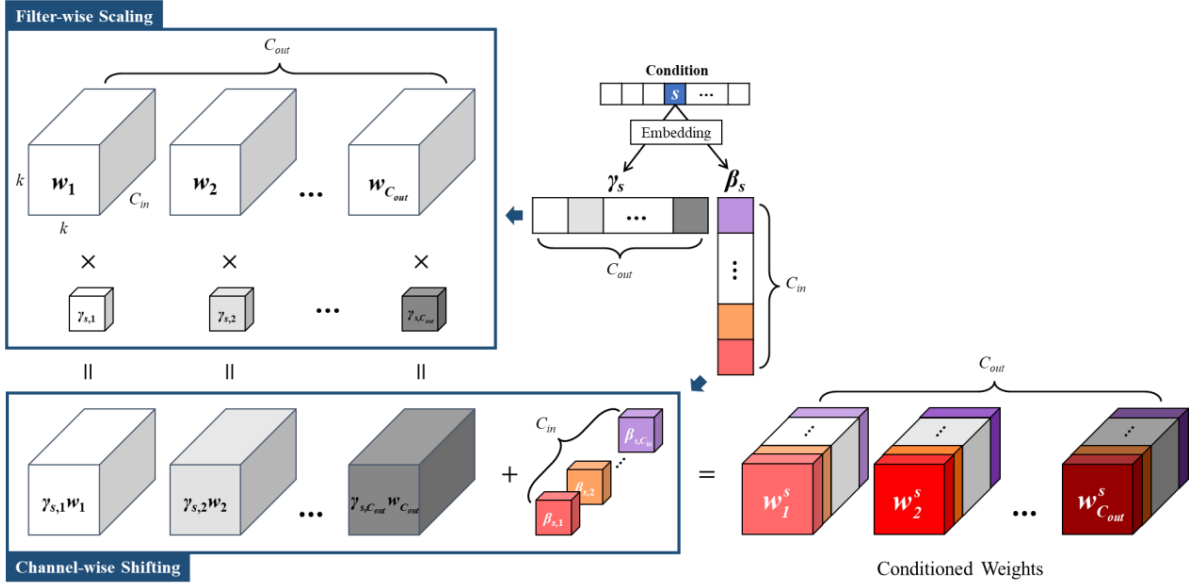


Fig. 3 Illustration of the proposed filter-wise scaling and the channel-wise shifting operations. By applying these operations, every filter and channel of the convolutional filters w are conditioned to a desired class with a small number of parameters.

where x , W , and \otimes indicate the input feature maps, convolution weights, and convolution operation, respectively. In addition, θ_s and δ_s are the scaling and shifting parameters, respectively, and these have different values according to the class label. By allowing the conditional information to manipulate the normalized feature maps, the cBN can conduct various conditional image generation tasks [2, 9, 15, 18]. However, one major drawback of the generator consisting of the cBN and standard convolution layer is that W in each convolution layer must handle the dynamic features of the whole class due to the fact that it is using the same W .

4 Proposed method

4.1 Conditional convolution layer

To cope with the aforementioned drawback, we propose a novel conditional convolution layer, called cConv, which produces the conditioned feature maps by employing the separated weights depending on the given condition. In general, the weights of the convolution layer are considered as a four-dimensional tensor $W \in \mathbb{R}^{k \times k \times C_{in} \times C_{out}}$, where k is the filter size, while C_{in} and C_{out} are the number of input and output channels, respectively. As shown in Fig. 3, each convolution layer has C_{out} filters with C_{in} channels. Each filter is denoted as $w_i, \{i = 1, \dots, C_{out}\}$. In order to produce conditioned weights $W^s \in \mathbb{R}^{k \times k \times C_{in} \times C_{out}}$, we modulate the W through filter-wise scaling and channel-wise shifting operations as follows: As shown in Fig. 3, we initially embed each

condition to specialized scaling parameters $\gamma_s \in \mathbb{R}^{C_{out}}$ and shifting parameters $\beta_s \in \mathbb{R}^{C_{in}}$. By using these parameters, we first conduct the filter-wise scaling operation on w_i with the scaling parameter $\gamma_{s,i}$ to individually provide the conditional information to each filter. Next, we apply the channel-wise shifting operation on the scaled w_i , which separately shifts each channel with shifting parameter $\beta_{s,j}$. This can be formally expressed as follows:

$$w_{i,j}^s = \gamma_{s,i} \cdot w_{i,j} + \beta_{s,j}, \quad \{i = 1, \dots, C_{out}, j = 1, \dots, C_{in}\} \quad (4)$$

where $w_{i,j}$ and $w_{i,j}^s$ indicate the j -th channel of the i -th filter in W and W^s , respectively. Note that the tensor broadcasting is included in (4). As shown in Fig. 3, with these sequential operations, all of the filters and channels of weights are specialized to a desired class with a small number of parameters. By utilizing W^s , the cConv can directly generate the conditioned feature maps without the need for conditional normalization process.

4.2 Understanding and analysis

In order to elucidate how W^s can effectively process the conditioned feature maps, we analyze the full operation of the cConv. As shown in Fig. 4, the output of the cConv y can be analyzed as follows:

$$y = x \otimes (\gamma_s W + \beta_s) = x \otimes \gamma_s W + x \otimes \beta_s. \quad (5)$$

Note that (5) includes tensor broadcasting to compute matrix operation. The first term $x \otimes \gamma_s W$ describes a

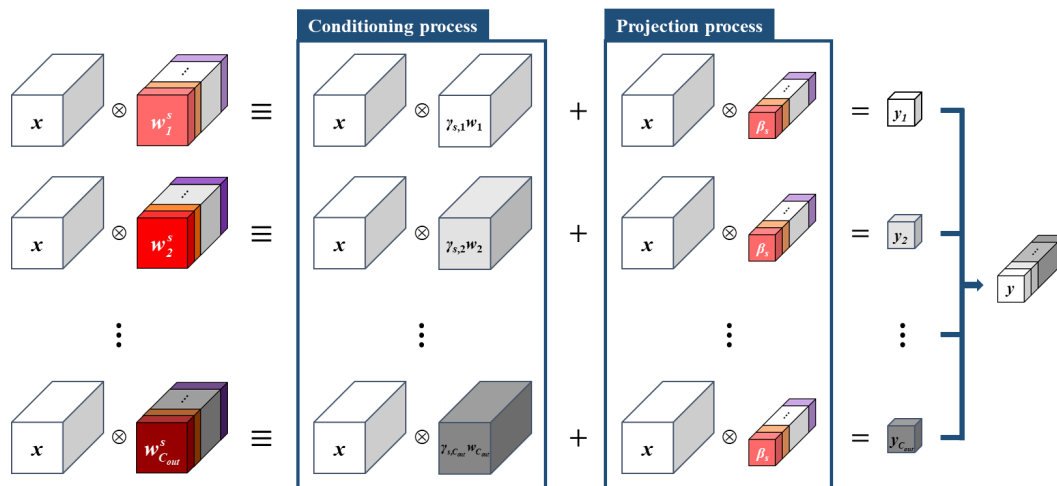


Fig. 4 Analysis of conditional convolution layer. The conditioned weights are divided into two terms, the conditioning and the projection processes. The conditioning process scales output feature maps with the specialized scale parameters corresponding to the condition. The projection process derives the condition-specific characteristics from the input feature maps and adds back to the output feature maps.

conditioning process which produces features that are scaled differently according to the given classes; this process helps disperse the convolutional feature maps. The second term $x \otimes \beta_s$ represents a *projection process* which derives the condition-specific components obtained by projecting x into β_s . These observations reveal that the proposed sequential operations not only directly produce the conditional feature maps but can also handle the dynamic features of various conditions.

In fact, more diverse W^s can be obtained by performing scaling and shifting operations with different values on each channel of every filter. However, this approach requires $2 \times N \times C_{in} \times C_{out}$ operating parameters in N conditions, which means the number of parameters rapidly increases with an increase in the dimension of the input and output feature maps. In contrast with this approach, although the proposed sequential modulation only requires $N \times (C_{in} + C_{out})$ parameters, it can specialize the weights to each condition. Therefore, with the advantages of simplicity and effectiveness, we adopt the proposed sequential operations to the cConv.

5 Experiments

5.1 Implementation details

In order to evaluate the superiority of the cConv, we conducted extensive experiments using the CIFAR-10 [23], CIFAR-100 [23], LSUN [25], and tiny-ImageNet [3, 24] datasets. The CIFAR-10 and CIFAR-100 datasets consist of 32×32 resolution images with 10 and 100 classes, respectively. The tiny-ImageNet and LSUN datasets con-

tain 10 and 200 classes of images, respectively, which have more detail and complex scenes. We compressed the images from the LSUN and tiny-ImageNet datasets as 128×128 pixels. For the objective function, we adopted the *hinge* version of adversarial loss which is defined as follow:

$$L_D = E_{(I,s) \sim P_{\text{data}}(I)}[\max(0, 1 - D(I, s))] + E_{z \sim P_z(z), s \sim P_{\text{data}}(s)}[\max(0, 1 + D(G(z, s)))] \quad (6)$$

$$L_G = -E_{z \sim P_z(z), s \sim P_{\text{data}}(s)} D(G(z, s)). \quad (7)$$

For all of the parameters in the generator and discriminator, we used the Adam optimizer [12] with a learning rate of 0.0002 and set the β_1 and β_2 to 0 and 0.9, respectively. We updated the discriminator five times per each update of the generator. For the CIFAR-10 and CIFAR-100 datasets, we used a batch size of 64 and trained the generator for 100k iterations, whereas the generator for the LSUN and tiny-ImageNet datasets was trained with a batch size of 32. Our experiments were conducted on CPU Intel(R) Xeon(R) CPU E3-1245 v5 and GPU TITAN X (Pascal), and implemented in *TensorFlow* v1.12.

5.2 Base lines

In order to evaluate the effectiveness of the proposed method, we employed the same generator and discriminator architectures as those used in the leading cGANs scheme [15]. The detailed architectures of the two different models for 32×32 and 128×128 resolutions are presented in Tables 1 and 2, respectively. Both of

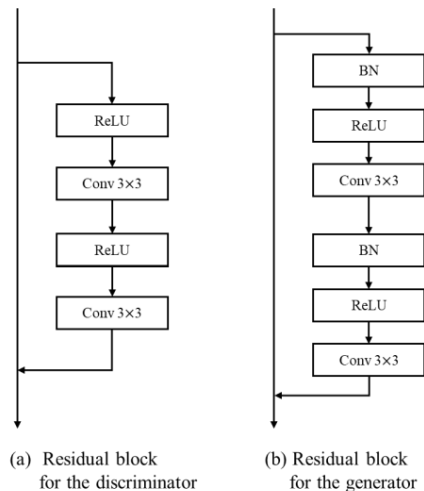


Fig. 5 Architecture of the ResBlock used in our experiments.

the models utilize the multiple residual blocks [6] (Res-Block) as illustrated in Fig. 5. Note that the discriminator does not contain the batch normalization (BN) layer since the spectral normalization [14] is applied to all of the weights in the discriminator. For the discriminator, we performed down-sampling (average-pooling) following the second convolutional layer in the ResBlock, whereas the generator up-sampled the feature maps using a nearest neighbor interpolation prior to the first convolution layer in the ResBlock.

5.3 Performance metrics

In order to evaluate how ‘realistic’ each generated image is, we employed the most popular assessments, inception score (IS) [21] and frechet inception distance (FID) [7], which measure the visual appearance and diversity of the generated images. The IS [21] computes the KL divergence between the conditional class distribution and marginal class distribution to measure the diversity and quality of the generated images. It is demonstrated in [21] that this metric is strongly correlated with the subjective human judgment of image quality. With a generated image X , the inception score can be defined as follows:

$$I = \exp(E[D_{KL}(p(n|X)||p(n))]), \quad (8)$$

where n is the label predicted by the Inception model [22], and $p(n|X)$ and $p(n)$ represent the conditional class distributions and marginal class distributions, respectively. With higher IS, the quality of the image generated from the model is higher. On the other hand, the FID is another assessment which is more principled and comprehensive. The FID can be obtained by calculating the Wasserstein-2 distance between the distribution of

$z \in \mathbb{R}^{128} \sim N(0, I)$	RGB image $x \in \mathbb{R}^{32 \times 32 \times 3}$
fully-connected, $4 \times 4 \times 256$	ResBlock, down sample, 128
ResBlock, up sample, 256	ResBlock, down sample, 128
ResBlock, up sample, 256	ResBlock, 128
ResBlock, up sample, 256	ResBlock, 128
BN, ReLU	ReLU
3 conv, 3, Tanh	Global sum pooling
	fully-connected, 1, projection

(a) Generator

(b) Discriminator

Table 1 Architectures of the generator and the discriminator used for the 32×32 CIFAR datasets. We follow the implementation of the Gulrajani *et al.* [6] in the same way as the leading cGANs framework [15]. (a) Architecture of the generator used for CIFAR datasets, (b) Architecture of the discriminator used for CIFAR datasets.

$z \in \mathbb{R}^{128} \sim N(0, I)$	RGB image $x \in \mathbb{R}^{32 \times 32 \times 3}$
fully-connected, $4 \times 4 \times 1024$	ResBlock, down sample, 64
ResBlock, up sample, 1024	ResBlock, down sample, 128
ResBlock, up sample, 512	ResBlock, down sample, 256
ResBlock, up sample, 256	ResBlock, down sample, 512
ResBlock, up sample, 128	ResBlock, down sample, 1024
ResBlock, up sample, 64	ResBlock, 1024
BN, ReLU	ReLU
3 conv, 3, Tanh	Global sum pooling
	fully-connected, 1, projection

(a) Generator

(b) Discriminator

Table 2 Architectures of the generator and the discriminator used for 128×128 LSUN and tiny-ImageNet datasets. (a) Architecture of the generator used for LSUN and tiny-ImageNet datasets, (b) Architecture of the discriminator used for LSUN and tiny-ImageNet datasets.

the generated samples, P_G , and the distribution of the real samples, P_R , in the feature space of the Inception model [22], which is expressed as follows:

$$F(p, q) = \|\mu_p - \mu_q\|_2^2 + \text{trace}(C_p + C_q - 2(C_p C_q)^{1/2}), \quad (9)$$

where $\{\mu_p, C_p\}$, $\{\mu_q, C_q\}$ are the mean and covariance of the samples with distribution P_G and P_R , respectively. In contrast with the IS, the generated samples with high quality have lower FID. In our experiments, we randomly generated 50,000 samples and computed the inception score and FID using the same number of real images.

5.4 Quantitative comparison

We conducted extensive experiments in order to demonstrate the advantage of the generator with the cConv over the two conventional conditioning methods: (i) input concat (*concat*) which provides the conditional information by concatenating the one-hot vector into the input noise, and (ii) conditional normalization (CN)

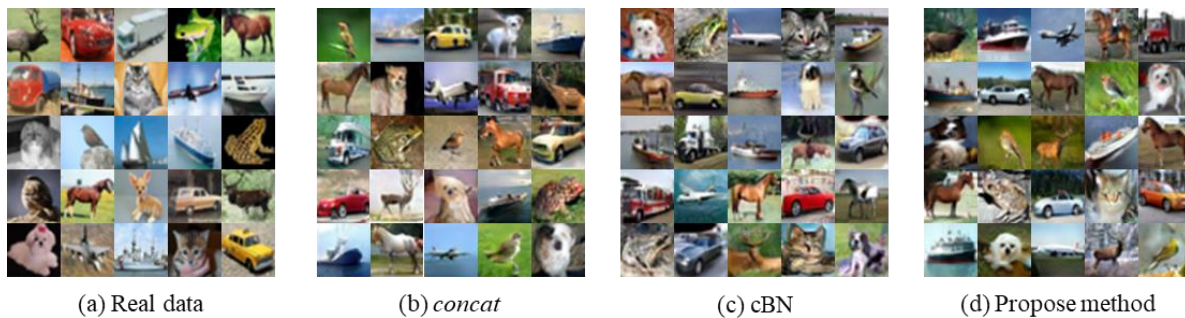


Fig. 6 Visual comparisons of the conventional and proposed methods on CIFAR-10 datasets. (a) The real data included in CIFAR-10, (b) Results of the *concat*, (c) Results of the CN [15], (d) Results of the proposed method.

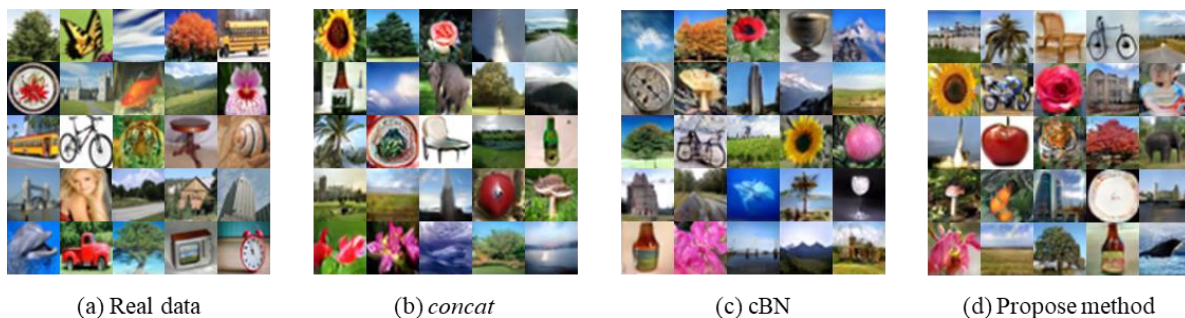


Fig. 7 Visual comparisons of the conventional methods and proposed method on CIFAR-100 datasets. (a) The real data included in CIFAR-100, (b) Results of the *concat*, (c) Results of the CN [15], (d) Results of the proposed method.

strategy which employs conditional batch normalization layer for the generator [15]. In the Resblock, the BN is replaced by the cBN for the CN experiments, and the standard convolution by the cConv for the experiments of the proposed method. In order to ensure fair comparison, both the proposed and conventional methods use the same projection discriminator [15].

Table 3 presents the comprehensive benchmarks between the proposed and conventional methods. The bold numbers in Table 3 indicate the best performance among the results. It is shown that the proposed method outperforms the *concat* by a considerable margin in terms of IS and FID. As compared with the CN, which has been known as the optimal solution to supply the conditional information to the generator [14, 15, 26], the proposed method shows better performance. Note that the cConv significantly improves the FID, which mainly evaluates the quality of the images, in the case of the CIFAR-100 dataset; this indicates that the cConv can successfully generate higher-quality images on many conditions than the conventional conditioning techniques.

In order to demonstrate the validity of the filter-wise scaling and the channel-wise shifting operations, we conducted ablation experiments by eliminating each operation from the cConv. Table 3 also shows that the cConv without the filter-wise scaling operation exhibits inferior performance on both datasets compared with

Method	Dataset			
	CIFAR-10		CIFAR-100	
	IS	FID	IS	FID
<i>concat</i>	8.21	14.51	8.67	16.06
CN [15]	8.45	11.12	8.99	15.58
cConv (proposed)	8.51	11.09	9.03	14.14
cConv*	8.31	13.48	8.05	20.59
cConv [†]	8.45	11.42	8.19	15.44

Table 3 Results of the quantitative assessments including IS and FID on both CIFAR-10 and CIFAR-100 datasets. * means proposed method without filter-wise scaling and [†] means proposed method without channel-wise shifting.

the cConv. These results show that the filter-wise scaling operation is very effective in producing the conditioned feature maps, resulting in the fact that the filter-wise scaling is an essential part of cConv to generate the conditioned feature maps. On the other hand, we observed that the cConv without the channel-wise shifting operation performs worse especially on the CIFAR-100 datasets. These results also indicate that the channel-wise shifting supports the derivation of conditional components for generating high-quality images in numerous conditions. Consequently, with a small number of parameters, both operations should be combined in order to maximize best performance of the cGANs scheme.

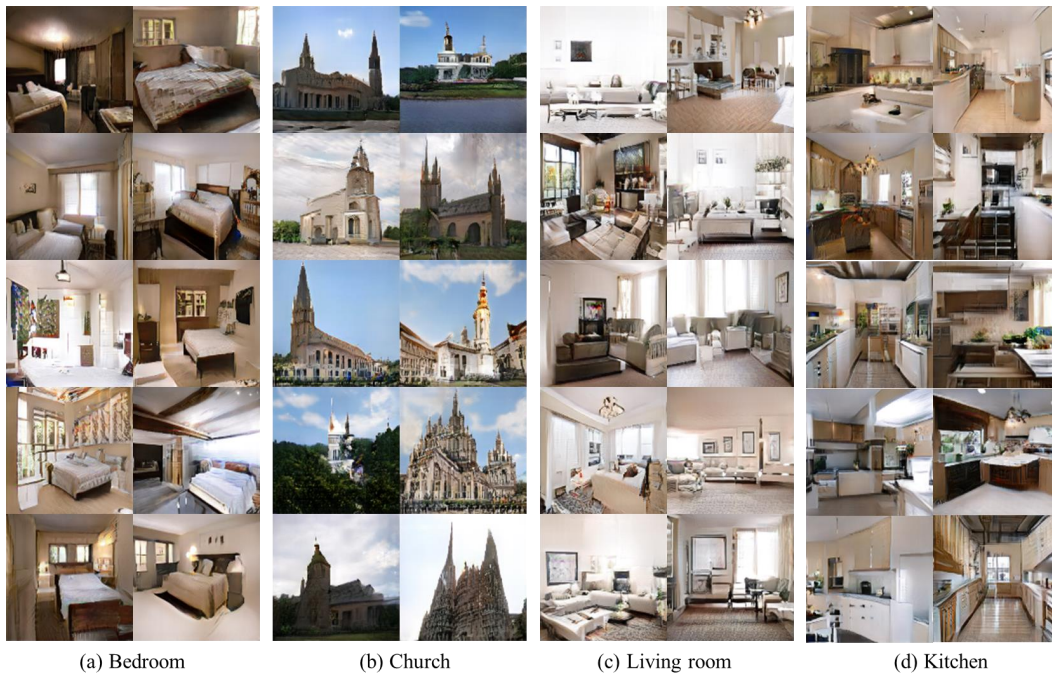


Fig. 8 128×128 pixel images generated with the proposed method using LSUN datasets.

Method	Dataset			
	CIFAR-10		CIFAR-100	
	IS	FID	IS	FID
<i>concat</i>	8.21	14.51	8.67	16.06
<i>concat</i> + cConv	8.47	10.90	8.65	15.04
CN [15]	8.45	11.12	8.99	15.58
CN + cConv	8.62	12.51	8.96	15.31

Table 4 Results of the combination of the proposed method with the conventional conditioning strategies on both the CIFAR-10 and CIFAR-100 datasets.

Furthermore, to validate the effectiveness of the proposed method, we built three types of generators which combine the proposed cConv with conventional conditioning methods as follow: (type I) the standard convolution + *concat* (or CN), (type II) the cConv + *concat* (or CN) and (type III) the cConv only. Table 4 shows that the method using the type II generator performs better than that using the type I generator. Consequently, the cConv is more suitable for handling the conditioned feature maps than the standard convolution layer. However, the performance of the model using the type II generator does not exceed that using the type III generator since the role of cConv is very similar to that of the conventional conditioning techniques.

5.5 Qualitative results

Conditional image generation Fig. 6 and Fig. 7 shows the generated images obtained using the aforementioned methods on the CIFAR-10 and CIFAR-100 data-sets. It can be seen that the resultant images obtained by the proposed method exhibit higher visual quality and fewer artifacts particularly for objects with complex shape such as bicycles in the CIFAR-100 dataset. In order to meaningfully demonstrate our results at higher resolution than CIFAR datasets, in addition, we conducted extra experiments on both LSUN [25] and tiny-ImageNet [3, 24] datasets which are considered to be more challenging ones consisting of detail and complex conditions. As shown in Fig. 8, the cConv can generate high-quality and diverse images including complex scenes with high resolution. Fig. 9(a) shows the samples for the classes with low FID, *i.e.*, classes on which the generative distribution is similar to the target conditional distribution, and Fig. 9(b) shows the reverse. As shown in Fig. 9(a), the images in the classes with low FID exhibit visually pleasing results with high diversity. However, as illustrated in Fig. 9(b), the images in the classes with high FID show slightly weak performance since they contain complex objects such as humans; that is, the diversity of the target data distribution is too wide. Note that this paper does not intend to design an optimal network structure for a generator with the cConv; there could be another architecture that leads to better performance. On the contrary, we



(a) Generated images on tiny-ImageNet with low FID



(b) Generated images on tiny-ImageNet with high FID

Fig. 9 128×128 pixel images generated with the cConv for the classes with (a) five low FID scores and (b) five high FID scores. The strings and values between each panel respectively indicate the name of the corresponding class and the FID score. The second row in each panel corresponds to the target dataset.

care more about whether it is possible to learn the conditioned feature maps by simply replacing the standard convolution layer with the proposed cConv.

Category morphing Using the proposed cConv, we can also successfully conduct category morphism. When there are two different conditions s_1 and s_2 , we simply inter-divide both filter-wise scaling and channel-wise shifting parameters of the cConv, corresponding to these conditions. Fig. 10 shows the interpolated images with the same input noise vector. Note that cConv can produce morphing images when s_1 and s_2 are significantly different.

5.6 Conditional image style transfer

In order to demonstrate the generalization ability of the cConv, we applied it to networks for the image style transfer task. In our experiments, we adopted the network architecture as well as the loss function presented in [11] to produce images in 10 different styles, including Yukiyo-e, Van gogh, and Jung-seob lee, using a single generator. Note that we replaced the standard convolutional layer of the generator with the cConv. Fig. 11 illustrates the results for a subset of the style. As shown in Fig. 11, the networks with cConv can provide the input images with different color palettes and textures



Fig. 10 The results of category morphing images obtained by using tiny-ImageNet datasets. The first row shows morphism from Alp to Seashore. The second row shows morphism from Beacon to Cliff.

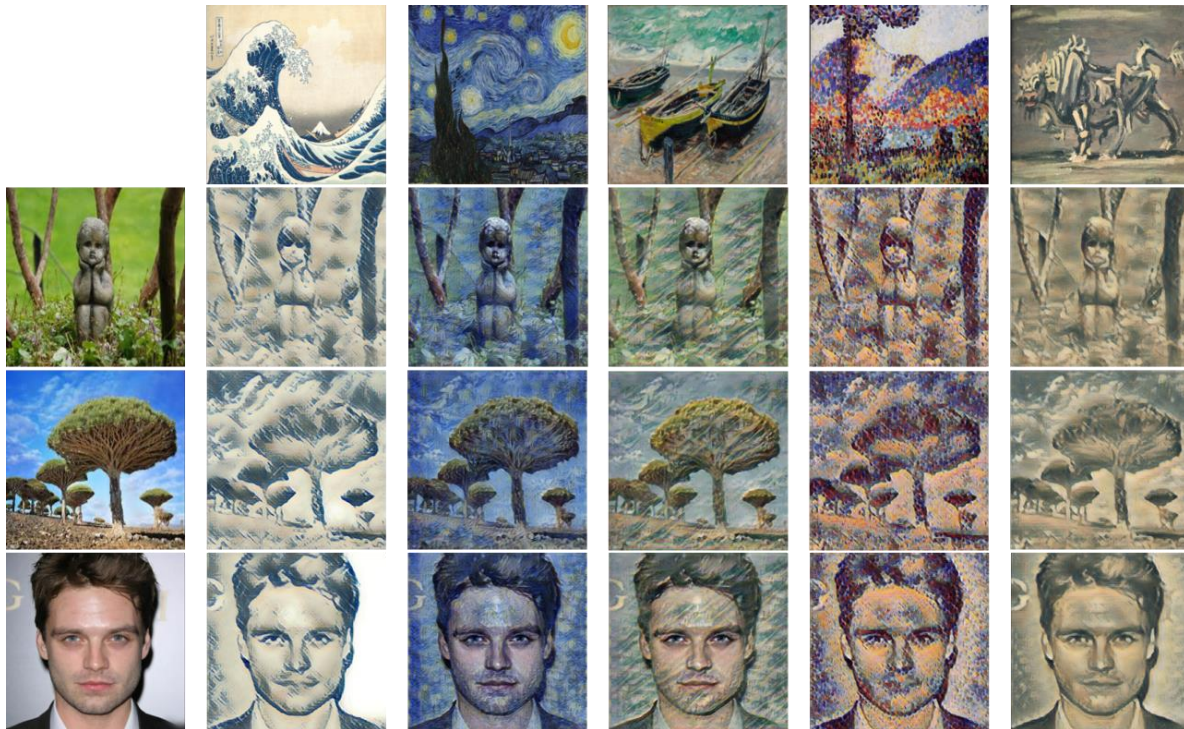


Fig. 11 The selected results of the conditional style transfer. Each row illustrates the resultant images with different artistic styles, which are Yukiyo-e, Van gogh, Claude monet, Henri edmond and Jung-seob lee, from the same input image.

depending on the given condition; the cConv can directly learn condition-wise features in each layer.

6 Conclusion

This paper presented a novel convolution layer, called a conditional convolutional layer, for cGANs. We demonstrated that the cConv can effectively handle the conditioned feature maps by applying the proposed filter-wise scaling and channel-wise shifting operations. One of the main advantages of cConv is that it can be incorporated into existing architectures, and our experiments reveal that the generator with the cConv significantly improves the performance of the baseline models. In addition, we proved the generalization ability of cConv by applying it to image style transfer. It is expected that the proposed method, with the advantage of simplicity and effectiveness, will be applicable to

other cGANs frameworks such as image-to-image translation and text-to-image synthesis.

References

1. Choi, Y., Choi, M., Kim, M., Ha, J.W., Kim, S., Choo, J.: Stargan: Unified generative adversarial networks for multi-domain image-to-image translation. In: Proceedings of the IEEE Conference on Computer Vision and Pattern Recognition, pp. 8789–8797 (2018) **1**
2. De Vries, H., Strub, F., Mary, J., Larochelle, H., Pietquin, O., Courville, A.C.: Modulating early visual processing by language. In: Advances in Neural Information Processing Systems, pp. 6594–6604 (2017) **4**
3. Deng, J., Dong, W., Socher, R., Li, L.J., Li, K., Fei-Fei, L.: Imagenet: A large-scale hierarchical image database. In: 2009 IEEE conference on computer vision and pattern recognition, pp. 248–255. Ieee (2009) **2, 5, 8**
4. Dumoulin, V., Shlens, J., Kudlur, M.: A learned representation for artistic style. Proc. of ICLR **2** (2017) **1, 2, 3**

5. Goodfellow, I., Pouget-Abadie, J., Mirza, M., Xu, B., Warde-Farley, D., Ozair, S., Courville, A., Bengio, Y.: Generative adversarial nets. In: *Advances in neural information processing systems*, pp. 2672–2680 (2014) [1](#), [3](#)
6. Gulrajani, I., Ahmed, F., Arjovsky, M., Dumoulin, V., Courville, A.C.: Improved training of wasserstein gans. In: *Advances in Neural Information Processing Systems*, pp. 5767–5777 (2017) [6](#)
7. Heusel, M., Ramsauer, H., Unterthiner, T., Nessler, B., Hochreiter, S.: Gans trained by a two time-scale update rule converge to a local nash equilibrium. In: *Advances in Neural Information Processing Systems*, pp. 6626–6637 (2017) [6](#)
8. Huang, X., Belongie, S.: Arbitrary style transfer in real-time with adaptive instance normalization. In: *Proceedings of the IEEE International Conference on Computer Vision*, pp. 1501–1510 (2017) [1](#), [2](#), [3](#)
9. Huang, X., Liu, M.Y., Belongie, S., Kautz, J.: Multi-modal unsupervised image-to-image translation. In: *Proceedings of the European Conference on Computer Vision (ECCV)*, pp. 172–189 (2018) [2](#), [4](#)
10. Isola, P., Zhu, J.Y., Zhou, T., Efros, A.A.: Image-to-image translation with conditional adversarial networks. In: *Proceedings of the IEEE conference on computer vision and pattern recognition*, pp. 1125–1134 (2017) [1](#)
11. Johnson, J., Alahi, A., Fei-Fei, L.: Perceptual losses for real-time style transfer and super-resolution. In: *European Conference on Computer Vision*, pp. 694–711. Springer (2016) [9](#)
12. Kingma, D.P., Ba, J.: Adam: A method for stochastic optimization. arXiv preprint arXiv:1412.6980 (2014) [5](#)
13. Mirza, M., Osindero, S.: Conditional generative adversarial nets. arXiv preprint arXiv:1411.1784 (2014) [1](#), [2](#), [3](#)
14. Miyato, T., Kataoka, T., Koyama, M., Yoshida, Y.: Spectral normalization for generative adversarial networks. arXiv preprint arXiv:1802.05957 (2018) [2](#), [3](#), [6](#), [7](#)
15. Miyato, T., Koyama, M.: cgans with projection discriminator. arXiv preprint arXiv:1802.05637 (2018) [1](#), [2](#), [3](#), [4](#), [5](#), [6](#), [7](#), [8](#)
16. Odena, A.: Semi-supervised learning with generative adversarial networks. arXiv preprint arXiv:1606.01583 (2016) [2](#), [3](#)
17. Odena, A., Olah, C., Shlens, J.: Conditional image synthesis with auxiliary classifier gans. In: *Proceedings of the 34th International Conference on Machine Learning-Volume 70*, pp. 2642–2651. JMLR. org (2017) [1](#), [2](#), [3](#)
18. Park, T., Liu, M.Y., Wang, T.C., Zhu, J.Y.: Semantic image synthesis with spatially-adaptive normalization. arXiv preprint arXiv:1903.07291 (2019) [4](#)
19. Reed, S., Akata, Z., Yan, X., Logeswaran, L., Schiele, B., Lee, H.: Generative adversarial text to image synthesis. arXiv preprint arXiv:1605.05396 (2016) [1](#), [2](#), [3](#)
20. Reed, S.E., Akata, Z., Mohan, S., Tenka, S., Schiele, B., Lee, H.: Learning what and where to draw. In: *Advances in Neural Information Processing Systems*, pp. 217–225 (2016) [1](#), [2](#), [3](#)
21. Salimans, T., Goodfellow, I., Zaremba, W., Cheung, V., Radford, A., Chen, X.: Improved techniques for training gans. In: *Advances in neural information processing systems*, pp. 2234–2242 (2016) [2](#), [3](#), [6](#)
22. Szegedy, C., Vanhoucke, V., Ioffe, S., Shlens, J., Wojna, Z.: Rethinking the inception architecture for computer vision. In: *Proceedings of the IEEE conference on computer vision and pattern recognition*, pp. 2818–2826 (2016) [6](#)
23. Torralba, A., Fergus, R., Freeman, W.T.: 80 million tiny images: A large data set for nonparametric object and scene recognition. *IEEE transactions on pattern analysis and machine intelligence* **30**(11), 1958–1970 (2008) [2](#), [5](#)
24. Yao, L., Miller, J.: Tiny imagenet classification with convolutional neural networks. *CS 231N* (2015) [2](#), [5](#), [8](#)
25. Yu, F., Zhang, Y., Song, S., Seff, A., Xiao, J.: Lsun: Construction of a large-scale image dataset using deep learning with humans in the loop. arXiv preprint arXiv:1506.03365 (2015) [2](#), [5](#), [8](#)
26. Zhang, H., Goodfellow, I., Metaxas, D., Odena, A.: Self-attention generative adversarial networks. arXiv preprint arXiv:1805.08318 (2018) [7](#)
27. Zhang, H., Xu, T., Li, H., Zhang, S., Wang, X., Huang, X., Metaxas, D.: Stackgan++: Realistic image synthesis with stacked generative adversarial networks. arXiv preprint arXiv:1710.10916 (2017) [1](#)
28. Zhang, H., Xu, T., Li, H., Zhang, S., Wang, X., Huang, X., Metaxas, D.N.: Stackgan: Text to photo-realistic image synthesis with stacked generative adversarial networks. In: *Proceedings of the IEEE International Conference on Computer Vision*, pp. 5907–5915 (2017) [3](#)
29. Zhu, J.Y., Park, T., Isola, P., Efros, A.A.: Unpaired image-to-image translation using cycle-consistent adversarial networks. In: *Proceedings of the IEEE international conference on computer vision*, pp. 2223–2232 (2017) [1](#)